3C.6 AFRICAN EASTERLY WAVE CONVECTION AND TROPICAL CYCLOGENESIS: A LAGRANGIAN PERSPECTIVE

Kenneth D. Leppert II * and Daniel J. Cecil
University of Alabama in Huntsville, Huntsville, Alabama

1. INTRODUCTION

African easterly waves (AEWs) have been shown to be important for tropical cyclogenesis in the Atlantic (e.g., Landsea 1993) and East Pacific (e.g., Avila 1991; Molinari and Vollaro 2000). In particular, these waves often provide a precursor low-level disturbance necessary for tropical cyclogenesis (Kurihara and Tuleya 1981). In addition, convection resident in AEWs may play an important role in tropical cyclogenesis via thermodynamic and dynamic feedbacks to the larger meso-to-synoptic scale circulation. For example, more widespread and/or intense convection could act to moisten mid and upper levels as a result of transport in convective updrafts. Strong, evaporatively-cooled downdrafts that can transport lower values of equivalent potential temperature (θ_e) towards the surface may be inhibited by this mid- to upper-level moistening, thus aiding tropical cyclogenesis (Rotunno and Emanuel 1987). By inhibiting strong downdrafts, the increase of mid- and upper-level moisture could also help to intensify updrafts and convection (e.g., Nolan 2007). This enhanced upward motion could aid the intensification and/or development of a mid- to low-level circulation (Nolan 2007; Raymond et al. 2011) via the stretching term in the vorticity equation. Thus, an enhancement of vorticity is another way convection could potentially aid tropical cyclogenesis.

The purpose of this study is to use a Lagrangian framework to analyze the evolution of and relation between AEWs, convection, and tropical cyclogenesis. In particular, we seek to determine the evolution of several convective characteristics (e.g., coverage and intensity) and the corresponding evolution of the thermodynamics and dynamics of larger-scale waves in the days leading up to and including tropical cyclogenesis. In the next section, a description of the methodology used is provided. Section 3 provides the main results from the study, and conclusions are given in section 4.

2. METHODOLOGY

Following the methodology of Leppert and Petersen (2010) easterly waves were analyzed and separated into ridge, northerly, trough, and southerly phases using NCEP-NCAR reanalysis (Kalnay et al. 1996) 700-hPa meridional wind data (note that the reanalysis has a spatial [temporal] resolution of 2.5° [six hours; averaged to one day for this study]) for June – November of 2001–2010 over a region stretching from 130°W –20°E (from the East Pacific to West Africa), 5°–20°N.

After the various wave phases were identified, information from National Hurricane Center (NHC) storm reports (NHC 2011) was utilized to identify AEW troughs that were associated with the development of a tropical cyclone of at least tropical storm strength (i.e., developing waves; DWs). NHC (2011) was also used to determine the day on which a tropical depression was first identified (i.e., day zero; D0) for each DW. Then each wave trough was traced up to five days prior to D0 (D-5) until one day after D0 (D+1). Any of the other three wave phases found within three data points (7.5°) east or west of the DW troughs were considered to be part of the DW.

In addition, we sought to compare the evolution of DWs with that of waves that never developed a tropical cyclone (i.e., nondeveloping waves; NDWs). Day zero for NDWs was defined as the day on which these waves achieved a maximum in 850-hPa vorticity within the trough phase. Presumably, the strongest, most coherent NDWs are most relevant for cyclogenesis. Hence, only those NDWs that could be tracked for at least seven days (NDWs were tracked manually using Hovmoller diagrams) and achieved a maximum 850-hPa vorticity of at least 8.0E-06 s^{-1} (equal to the mean 850-hPa vorticity of all NDW troughs plus one standard deviation; for comparison, the mean 850-hPa trough vorticity of DWs on D0 is 5.1E-06 s^{-1}) were included in the analysis. Once D0 for NDW troughs was identified, other days relative to D0 as well as other wave phases were identified for NDWs as they were for DWs.

Using a similar methodology to that used by Hopsch et al. (2010), composites of several large-scale variables, including θ_e and vorticity, were created as a function of wave phase and day relative to D0 for all DWs and NDWs using data taken from the NCEP-NCAR reanalysis dataset. These composites were used to assess the evolution of the large-scale wave circulation and structure.

In order to assess the evolution of the coverage by cold cloudiness associated with easterly waves, the 4-km IR brightness temperatures from the NASA global-merged IR brightness temperature dataset (Liu et al. 2009) were utilized. In particular, the IR brightness temperatures were used to find the fraction of each 2.5° box covered by temperatures ≤210 K and ≤240 K. These areal coverage fractions were subsequently composited similar to the large-scale reanalysis variables.

Several different datasets were used to assess the intensity of convection and its associated evolution including lightning data from the lightning imaging sensor (LIS; Boccippio et al. 2002; flash rates valid for

* *Corresponding author address*: Kenneth D. Leppert II, NSSTC, 320 Sparkman Dr., Rm 4074, Huntsville, AL 35805; e-mail: leppert@nsstc.uah.edu.

each day and 2.5° grid box were calculated and then composited similar to other variables) on board the Tropical Rainfall Measurement Mission (TRMM) satellite, radar reflectivity data from the TRMM precipitation radar (PR; Kummerow et al. 1998), and 37.0/85.5-GHz brightness temperatures from the TRMM microwave imager (TMI; Kummerow et al. 1998).

3. RESULTS

Some waves may have developed a tropical cyclone and/or achieved their maximum low-level vorticity close to the West African coast or the west coast of Central America. Hence, the evolution of some easterly waves from D-5 to D0 includes a transition from over land to ocean. Because convective intensity and lightning generally decrease over the ocean compared to land (e.g., Toracinta et al. 2002; Christian et al. 2003), it is possible that a decrease in the intensity of convection may be observed for waves as they evolve from D-5 to D0 unrelated to the evolution towards cyclogenesis. Therefore, a land mask was applied to all composites.

The composite coverage by IR brightness temperatures ≤240 K provided in Table 1 (as a function of wave phase and day relative to D0) indicate that the trends in coverage by cold cloudiness vary as a function of phase in the days leading up to tropical cyclogenesis for DWs. For example, the coverage increases from D-5 until D-2 in the ridge and northerly phases and then decreases thereafter. In contrast, the coverage generally increases from D-5 to D0 in the trough and southerly phases (note that coverage decreases on D+1 in these wave phases). The IR threshold values for NDWs provided in Table 1 suggest an evolution of the coverage by cold cloudiness that is similar to that of DWs. In particular, the NDW ridge phase shows much variability in coverage from D-5 to D+1 while the other phases show a general increasing trend on all days except D+1. While the evolution of coverage by cold cloud tops is similar between DWs and NDWs, the magnitude of values are significantly greater (i.e., statistical significance at the 99% level using the analysis of variance technique) for DWs on nearly all days and in all phases, except the ridge phase. Hence, it appears that a greater coverage by cold cloudiness is more relevant to tropical cyclogenesis than the evolution of that coverage in the days leading up to genesis.

In contrast to what is observed for the coverage by cold cloudiness (especially in the trough and southerly phases), the intensity of DW convection as indicated by composite lightning flash rates (Fig. 1a) appears to decrease as D0 is approached. Specifically, both the trough and southerly phases show a decrease in flash rate every day after D-4. The northerly and ridge phase values vary from day to day, but flash rates in both phases decrease by more than 60% from D-5 until D0.

The LIS flash rates of NDWs shown in Fig. 1b show much variability from day to day with little indication of any consistent trends. However, the flash rates of all NDW phases are greater on D0 and D+1 when compared to the corresponding values on D-5, suggesting an increase in intensity with time for these waves or, at least, a constant intensity with time (it is possible that more flashes are recorded by LIS due to the increasing coverage by [potentially electrically-active] cold cloudiness with time, giving the impression of an increasing flash rate with time while the flash rate [i.e., intensity] of individual convective elements does not change), in contrast to DWs which show a decrease in lightning with time despite an increase in coverage of cold cloudiness. Note, however, that any trends in lightning flash rates observed for either DWs or NDWs are small compared to the standard deviation of 144.5 flashes day^{-1}.

Another difference between DWs and NDWs can be observed in the evolution of large-scale profiles of the θ_e anomaly shown in Fig. 2 as a function of day relative to D0 for the trough phase. The DWs show a consistent increase in moisture throughout a large depth of the troposphere on nearly all days, while NDWs only show an increase on some days over a relatively

Table 1. The fraction of a 2.5° by 2.5° grid box (76176 km^2) covered by IR brightness temperatures less than or equal to 240 K as a function of wave phase and day relative to D0 for developing and nondeveloping waves (a land mask has been applied to both wave types). The values are valid from five days prior to D0 (D-5) to one day after D0 (D+1). The bold numbers indicate values that are statistically significantly (at the 99% level) greater than the corresponding values of the other wave category based on the analysis of variance technique, and italics indicate values that are significantly greater than the value from the previous day from the same wave type and phase.

Developing Waves

Day	*Ridge*	*Northerly*	*Trough*	*Southerly*
D-5	0.094	**0.100**	**0.112**	0.090
D-4	**0.102**	**0.107**	**0.122**	*0.112*
D-3	**0.105**	**0.124**	**0.121**	**0.118**
D-2	0.107	**0.137**	***0.146***	***0.143***
D-1	0.102	**0.132**	**0.152**	***0.170***
D0	0.096	0.114	**0.171**	**0.177**
D+1	0.088	0.100	**0.163**	**0.161**

Nondeveloping Waves

D-5	0.068	0.054	0.076	0.096
D-4	0.064	0.066	0.067	0.103
D-3	0.067	0.075	0.070	0.084
D-2	0.100	0.093	*0.098*	0.094
D-1	0.112	0.105	*0.125*	0.107
D0	0.103	0.117	0.139	0.123
D+1	0.096	0.082	0.113	0.108

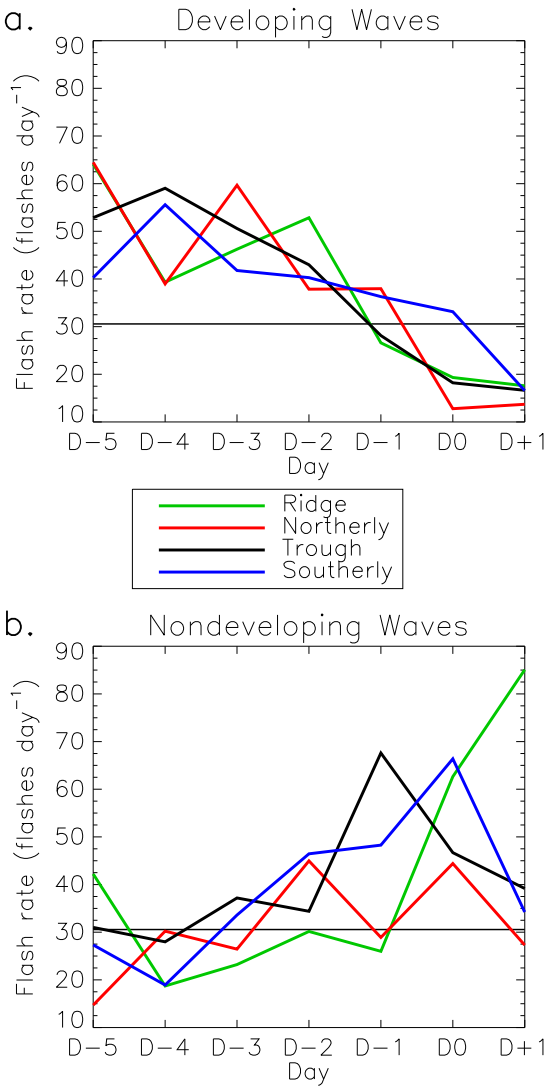

Fig. 1. Composite lightning flash rates as a function of day relative to D0 for each wave phase of a.) developing waves and b.) nondeveloping waves after application of a land mask. Note that the labels along the abscissa are for five days prior to D0 (D-5) to one day after D0 (D+1). The thin, horizontal lines indicate the average flash rate over the full analysis domain, and the standard deviation is 144.5 flashes day^{-1}.

shallow depth. In addition, the θ_e anomaly is greater for DWs compared to NDWs on nearly all days and levels.

Some differences are also observed between DWs and NDWs in terms of the evolution of the large-scale wave circulation as shown in Fig. 3 by composite profiles of relative vorticity for the trough phase of each wave type. In particular, DWs are associated with an increase in cyclonic vorticity at midlevels (~500–600 hPa) on D-1 and a subsequent increase between ~500–

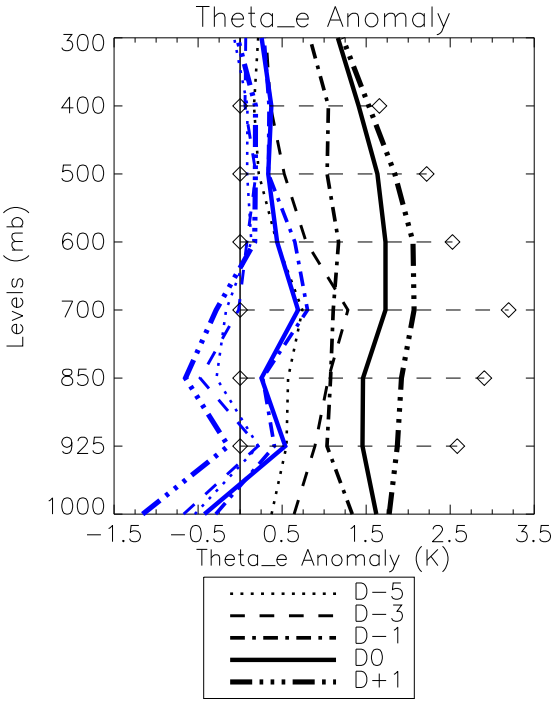

Fig. 2. Composite analysis of vertical profiles of the θ_e anomaly (anomaly relative to the mean at each pressure level and longitude) as a function of day relative to D0 for the trough phase (a land mask has been applied). The black (blue) lines are for developing waves (nondeveloping waves). The profiles are valid for five days prior to D0 (D-5) to one day after D0 (D+1; note that the D-4 and D-2 profiles are not shown for clarity), and the horizontal dashed lines indicate the value of the standard deviation at each level.

1000 hPa on D0 and D+1 (although, these increases are admittedly small). Note that the initial increase in midlevel vorticity for DWs appears to be consistent with several previous studies (e.g., Nolan 2007; Raymond et al. 2011). In contrast, NDWs show an increase in cyclonic vorticity below 500 hPa on D-1 and D0 with a subsequent decrease on D+1. Note in particular the large increase in 850-hPa vorticity for NDWs on D0, which, of course, is due to how D0 is defined for NDWs. At upper levels (~200 hPa), DWs exhibit an increase in anticyclonic vorticity on all days except D+1 (NDWs are associated with an increase in upper-level anticyclonic vorticity until D-1 that remains nearly constant thereafter). The development of greater upper-level anticyclonic vorticity for DWs combined with the increase in mid- and low-level cyclonic vorticity suggests the development of a warm core in association with thermal wind balance, consistent with tropical cyclogenesis.

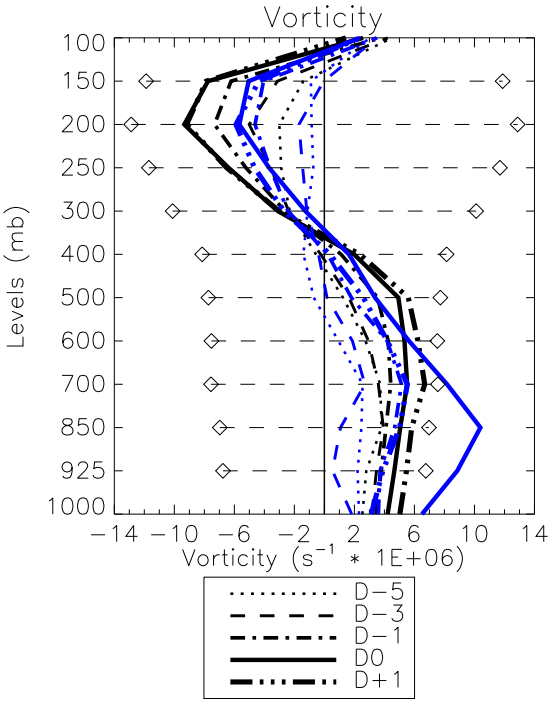

Fig. 3. As in Fig. 2, except for vertical profiles of relative vorticity. The horizontal dashed lines indicate ± one standard deviation.

4. CONCLUSIONS

Results suggest that the coverage by cold cloudiness increases as D0 is approached for DWs, in particular within the trough and southerly phases, while the intensity of convection appears to decrease with time in all DW phases. The evolution of NDWs also generally shows an increase in coverage by cold cloudiness as D0 is approached, but convective intensity appears to remain approximately constant with time, perhaps increasing slightly. In addition, the coverage by cold cloudiness is generally always greater for DWs. In terms of large-scale wave structure, DWs are associated with more moisture than NDWs. Hence, results suggest that the most important characteristics for tropical cyclogenesis and distinguishing DWs from NDWs is a greater coverage by cold cloud tops and enhanced large-scale moisture.

5. REFERENCES

Avila, L. A., 1991: Eastern North Pacific hurricane season of 1990. *Mon. Wea. Rev.*, **119**, 2034−2046.

Boccippio, D. J., W. J. Koshak, and R. J. Blakeslee, 2002: Performance assessment of the optical transient detector and lightning imaging sensor. Part I: Predicted diurnal variability. *J. Atmos. Oceanic Technol.*, **19**, 1318–1332.

Christian, H. J., and Coauthors, 2003: Global frequency and distribution of lightning as observed from space by the optical transient detector. *J. Geophys. Res.*, **108**, 4005, doi:10.1029/2002JD002347.

Hopsch, S. B., C. D. Thorncroft, and K. R. Tyle, 2010: Analysis of African easterly wave structures and their role in influencing tropical cyclogenesis. *Mon. Wea. Rev.*, **138**, 1399–1419.

Kalnay, E., and Coauthors, 1996: The NCEP/NCAR 40-year reanalysis project. *Bull. Amer. Meteor. Soc.*, **77**, 437–471.

Kummerow, C., W. Barnes, T. Kozu, J. Shiue, and J. Simpson, 1998: The tropical rainfall measuring mission (TRMM) sensor package. *J. Atmos. Oceanic Technol.*, **15**, 809–817.

Kurihara, Y., and R. E. Tuleya, 1981: A numerical simulation study on the genesis of a tropical storm. *Mon. Wea. Rev.*, **109**, 1629–1653.

Landsea, C. W., 1993: A climatology of intense (or major) Atlantic hurricanes. *Mon. Wea. Rev.*, **121**, 1703–1713.

Leppert, K. D., II, and W. A. Petersen, 2010: Electrically-active hot towers in African easterly waves prior to tropical cyclogenesis. *Mon. Wea. Rev.*, **138**, 663−687.

Liu, Z., D. Ostrenga, G. G. Leptoukh, and A. V. Mehta, 2009: Online visualization and analysis of global half-hourly pixel-resolution infrared dataset. *Extended Abstracts, 25th Conf. on International Interactive Information and Processing Systems (IIPS) for Meteorology, Oceanography, and Hydrology*, Phoenix, AZ, Amer. Meteor. Soc., J3.4.

Molinari, J., and D. Vollaro, 2000: Planetary- and synoptic-scale influences on Eastern Pacific tropical cyclogenesis. *Mon. Wea. Rev.*, **128**, 3296–3307.

National Hurricane Center, cited 2011: NHC archive of hurricane seasons. [Available online at http://www.nhc.noaa.gov/pastall.shtml.]

Nolan, D. S., 2007: What is the trigger for tropical cyclogenesis? *Aust. Meteorol. Mag.*, **56**, 241–266.

Raymond, D. J., S. L. Sessions, and C. Lopez Carrillo, 2011: Thermodynamics of tropical cyclogenesis in the northwest Pacific. *J. Geophys. Res.*, **116**, D18101, doi:10.1029/2011JD015624.

Rotunno, R., and K. A. Emanuel, 1987: An air–sea interaction theory for tropical cyclones. Part II: Evolutionary study using a non-hydrostatic axisymmetric numerical model. *J. Atmos. Sci.*, **44**, 542–561.

Toracinta, E. R., D. J. Cecil, E. J. Zipser, and S. W. Nesbitt, 2002: Radar, passive microwave, and lightning characteristics of precipitating systems in the tropics. *Mon. Wea. Rev.*, **130**, 802–824.